Article type:

Corresponding author: Milan Pecanac, pecanac.milan@uns.ac.rs

Knoop Hardness Optimal Loading in Measuring Microhardness of Maraging Steel Obtained by Selective Laser Melting

Sebastian Balos[1], Dragan Rajnovic[1], Leposava Sidjanin[1], Snezana Ciric Kostic[2], Nebojsa Bogojevic[2], Milan Pecanac[1*], Jelena Pavlicevic[3]

[1] Faculty of Technical Sciences, University of Novi Sad, 21000 Novi Sad, Serbia

[2] Faculty of Mechanical and Civil Engineering in Kraljevo, University of Kragujevac, Dositejeva 19, 36000 Kraljevo, Serbia

[3] Faculty of Technology, University of Novi Sad, 21000 Novi Sad, Serbia

Abstract

Knoop microhardness methods possesses several advantages over Vickers testing: lower penetration depth, higher accuracy in indentation measurement and a better suitability to measuring thin and elongated morphological features. This study explores the optimal loading and load independent hardness of selective laser melted specimens in non-heat-treated and heat-treated conditions, by using different Knoop test loads. The obtained results were used to plot load to indentation size charts, which, in turn, were used to obtain prediction curves in accordance to Meyer, PSR and modified PSR models. The fitting of fitting curves to the measured values was used to calculate appropriate correlation factors. The results indicate that indentation size effect occurs in all measured specimens. This suggests that there is material true microhardness. Also, the most adequate model was modified PSR, with correlation factors just under one.

Key words

Selective laser melting, Knoop microhardness, Indentation size effect, Load independent hardness

Introduction

Direct Selective Laser Sintering (DSLS) or Selective Laser Melting (SLM) technique are additive fabrication methods, which can be used to produce three-dimensional parts. This is done without binder, by a direct effect of laser joining of several tens of microns powder [1]. SLM technology offers huge advantages in flexibility over conventional technologies such as machining, casting and joining of cast, hot or cold-rolled profiles, especially when fabricating complex and thin-walled three-dimensional parts [2, 3]. Furthermore, this technology offers a high flexibility regarding materials used as well, ranging from metallic materials such as different types of steels, titanium, aluminum, nickel and other alloys, extending to various

ceramics and polymers [4–11]. On the other hand, a wider industrial application is hindered by certain disadvantages, ranging from the occurrence of residual stresses, particularly of tensile nature leading to a possible cracking, distortion, porosity that can trigger crack nucleation, all leading to lower mechanical properties than those of conventionally produced parts. To overcome these deficiencies, a comprehensive optimization is needed, as well as modifications to the basic SLM principle, such as the tailoring of residual stresses by Laser Shot Peening (LSP), increasing mechanical properties, most notably, fatigue resistance [12–14]. Other measures are controlling the temperature of the build plate as well as applying post-fusion treatments as polishing and aging [15, 16]. Together with the attempts of increasing mechanical properties, the development of characterization techniques is necessary. One of the quickest and simplest is hardness or microhardness measurement. However, there is hardly a firm agreement which technique is best suited to additive manufactured (AM) parts. AM parts differ from machined, welded or cast parts in their inherent non-homogeneity throughout the cross section, containing a number of heat affected-zones around locally melted and crystallized material [17, 18]. This is a direct consequence of the build direction and cross section direction, revealing the laser pattern used for powder fuse [19]. Therefore, it is of utmost importance to optimize hardness measurement process to obtain valid results. Different researchers used various hardness measurement techniques to assess the performance of the AM fabricated parts. The majority of researchers use the Vickers microhardness technique, but with various loadings applied on the diamond indentor [20–23]. However, in the research done by Nie et al. [24], Knoop method was used to determine the microhardness of fused iron and tungsten specimens obtained by SLM. Although Vickers and Knoop microhardness methods use virtually the same principle, compared to Vickers microhardness, Knoop method uses an elongated pyramidal diamond indenter that provides several specific features. Knoop indenter penetration depth is lower compared to Vickers indenter when the same loading is applied. This makes Knoop microhardness better suited to high hardness brittle materials. Also, Knoop test is more sensitive to the irregularities on the surface of the specimen, as well as better suited to multilayer materials, where the effect of the bottom layer is lower or non-existent. Knoop major diagonal is approximately three times longer than Vickers diagonals, leading to a higher accuracy of the measurement particularly of small indents. Knoop test is better suited to elongated areas, while Vickers test of rounded areas [25]. Both types of areas exist in SLM, making both tests viable.

In this study, an attempt was made to use Knoop test for measuring the microhardness of SML manufactured specimens of MS1 maraging steels in different conditions. A special attention was payed to the indentation size effect (ISE) obtained by applying different loadings. Namely, The ISE is indentation-depth-dependent hardness, which can be influenced by dislocation movement, that is, deformation mechanisms, material roughness, etc. [26–28]. According to Dobransky different loadings will be applied to measure Knoop microhardness of MS1 steel [29]. The aim is to obtain Knoop Load Independent Hardness (H_{LIH}) of the material as a reference for future studies

Experimental

The subject of Knoop microhardness testing and further microstructure analysis were cylindrical specimens built in vertical position, with a diameter of 8 mm and the length of 50 mm which were produced by the Selective Laser Melting (SLM) technology. The SLM process was done in the 3D Impulse Center of the Faculty of Mechanical and Civil Engineering in Kraljevo, Serbia. The SLM device used for fabricating samples was EOSINT

M280. Following parameters of SLM were: Ytterbium laser, with 0.2032 mm thick 1064 nm beam was used in nitrogen gas environment at a power of 200 W. During SLM fabrication, the material is built up in layers with a layer thickness of 40μm. After fusing, the specimen surfaces were cleaned by microshot-peening by 0.4 mm stainless steel balls. Half of the specimens were left untreated (designated as N) and the other half was heat treated by aging at 490°C for 6 h (designated as H) as recommended by manufacturer of the powder. The used material was MS1 margining steel ("18%Ni Maraging 300") with chemical composition shown in Table 1 obtained by the authors from paper [19] as a collaboration.
SEM micrographs of the atomized powder are presented in Figure 1. The material is well atomized without large amounts of satellites, fused/bonded particles or inhomogeneity. The size of MS1 powder ranges from 1 to 42 μm with an average size around 26.21 μm.

Table 1 Steel powder composition [mass. %] [19]

Ni	Co	Mo	Ti	Al	Cr	Cu	C	Mn	Si	P, S	Fe
17.58	9.26	4.51	0.72	0.13	0.24	0.24	0.028	0.041	0.06	0.012	balance

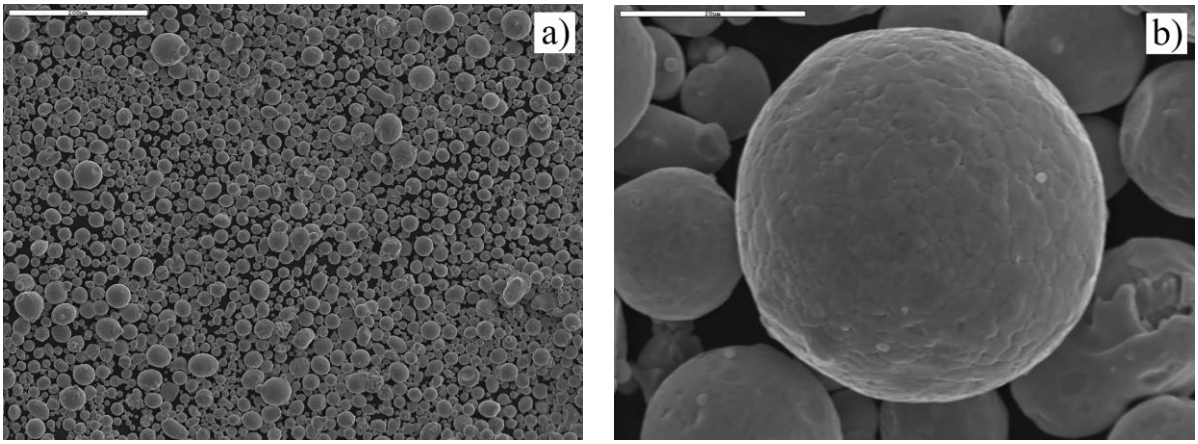

Figure 1. SEM micrograph, showing the morphology of MS1 powder

In this study the characterization techniques comprised of microstructure examination and microhardness measurement, were applied in two planes, longitudinal and cross section plane on the specimens used. Microstructure examination was conducted after standard metallographic preparation on Struers equipment and Aqua regia etching. The evaluation of microstructures was done on Leitz Orthoplan light microscope (LM). Microhardness was measured by Knoop method, using the Wilson Tukon 1102 device at different loads: 10, 25, 50, 100, 200, 300, 500 and 1000 g; was performed in accordance with ASTM E 384-08 [30]. Each reported value represents an average of three measurements.
To distinguish the specimens, the designation system was devised: non-heat-treated specimen cut longitudinally (NL), non-heat-treated cross-sectioned (NC), heat treated cut longitudinally (HL) and heat-treated cross-sectioned (HC). The surface morphologies on longitudinal and cross section are shown in Fig. 2. In longitudinal cross-section a scale-like melted areas are present (Fig. 2a, c) while in cross-section an elongated melted area could be observed (Fig. 2b, d)

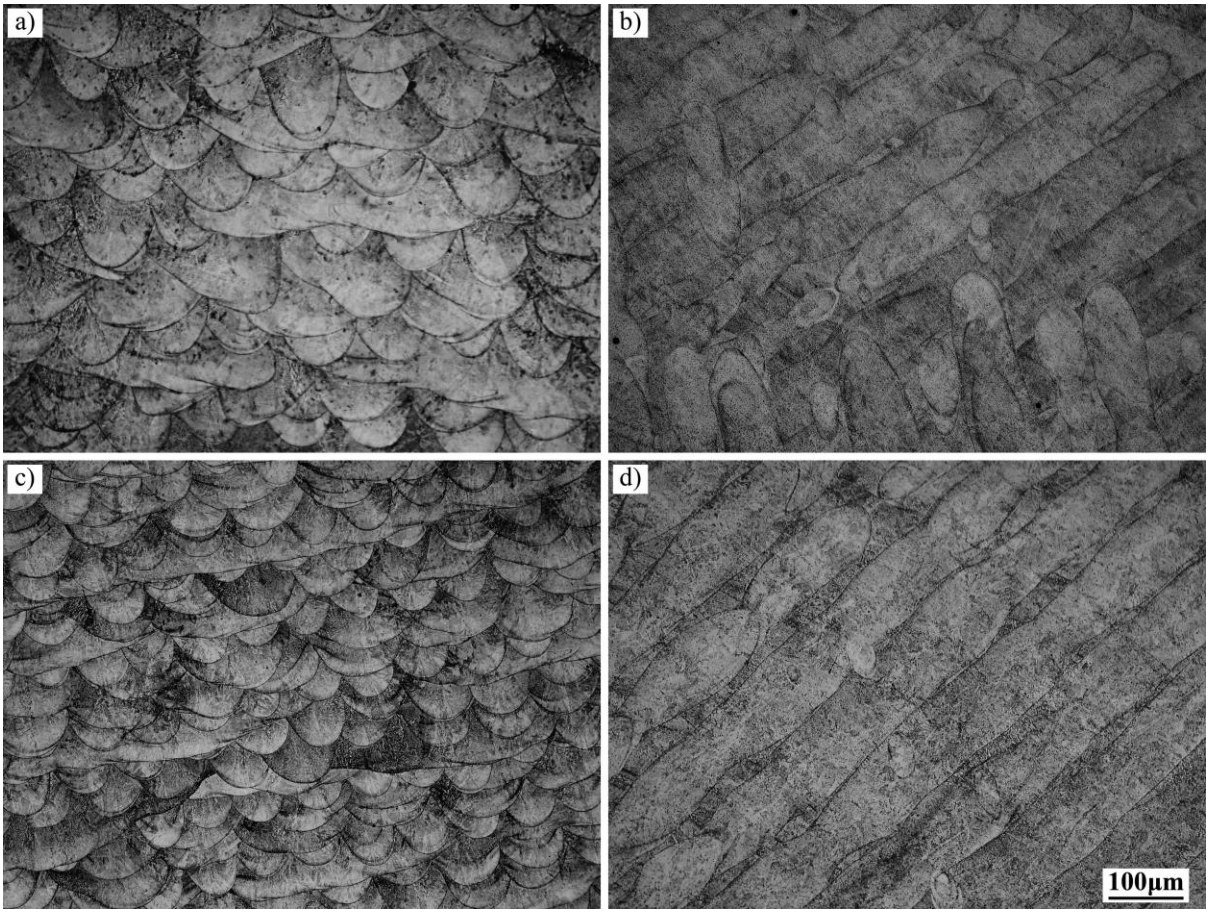

Figure 2. Surface morphologies of SLM manufactured specimens: a) NL; b) NC; c) HL; d) HC (LM)

Results and Discussion

The Knoop microhardness values in relation to indentation load, obtained on specimens NL, NC, HL and HC, are presented in Fig. 3. Based on shown trends, as the loading increases, Knoop microhardness values decrease. At indentation loadings over 2.9 N, the trend exponentially reaches an almost constant value. For non-heat-treated specimens (NL, NC), this constant value is around 400 HK, while for heat-treated specimens (HL, HC), the value approaches 600 HK. These values can be the so-called load independent hardness (H_{LIH}).

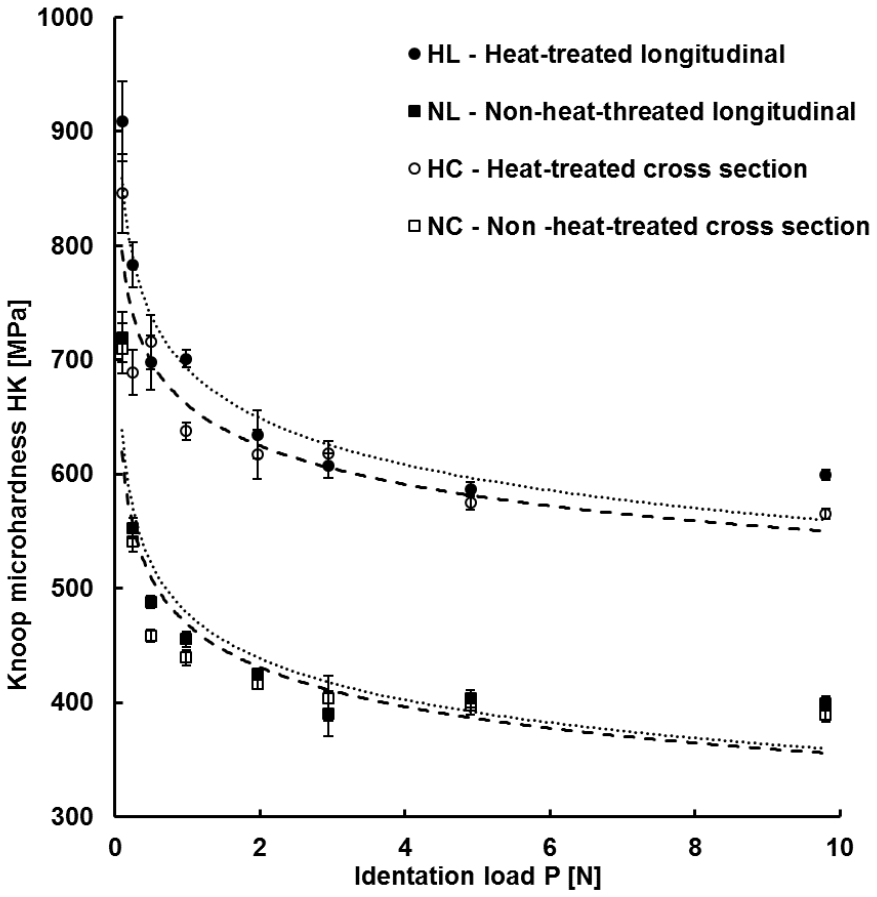

Figure 3. Knoop microhardness values in relation to indentation load

The quantitative description of the experimental Knoop microhardness values can be conducted by correlation models by classical Meyer's law, PSR model and modified PSR model. Meyer's law has the form as in Equation 1:

$$P=Ad^n \quad (1)$$

where P is the indentation load and d the resulting indentation size, while A and n are values derived from the fitting curves of the indentation load to indentation size dependencies [31]. The results of application of equation 1 are shown in Table 2 and Figure 4. It can be seen that the exponent n is higher in specimens HL and HC, indicating a marginally less pronounced indentation size effect in these specimens, compared to NL and NC. This is in accordance to the curves shown in Fig. 4. Also, a slightly higher correlation factors are obtained for specimens NC and HC (cross-sectioned) compared to specimens NL and HL (sectioned longitudinally). This is understandable since in specimens NC and HC, the elongated melted areas are revealed, versus scale-like melted areas in specimens NL and HL.

Table 2 Regression analysis results of the experimental data in accordance to Meyer's law

Specimen	A	log A	n	R^2
NL	16168	4.208656	1.7364	0.9939
NC	17417	4.240973	1.7758	0.9989
HL	28689	4.457715	1.8294	0.9993
HC	29184	4.465145	1.8478	0.9994

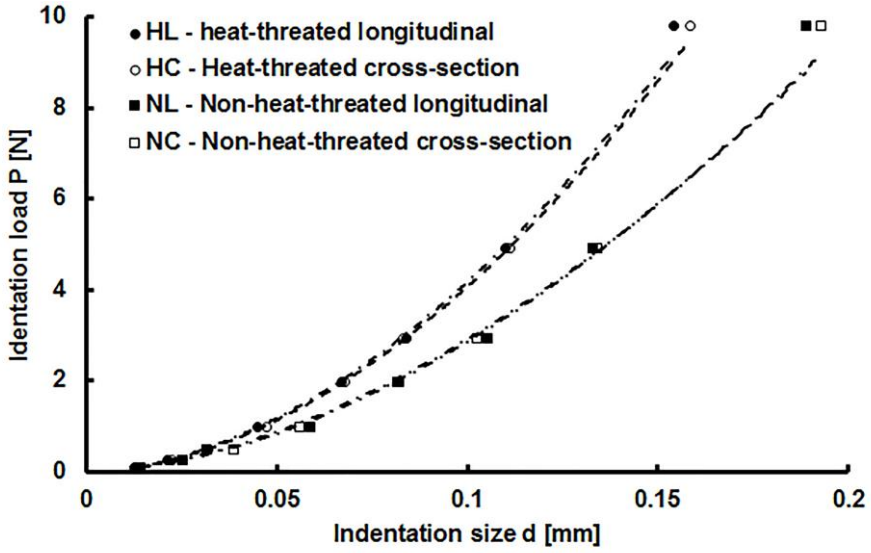

Figure 4. Indentation load versus indentation size according to Meyer's law

Proportional specimen resistance (PSR) model based on the equation (2) [32]:

$$P=a_1d+a_2d^2 \quad (2)$$

where a_1 and a_2 are experimental constants obtained from the fitting curve. The parameters a_1 and a_2 are constant for given material and can be related to the elastic and plastic properties of the test material, respectively [32]. The results of regression analysis in accordance to PSR model are shown in Table 3 and Fig. 5. It can be seen that similar correlation factors (R^2) are obtained, as by using the Meyer's model. Presence of surface stress is evident in case of cross-sectioned samples (NC and HC) with negative values of P_0, while in longitudinal plane (NL and HL) a higher plasticity of surface could be observed.

Table 3 Regression analysis results of the experimental data in accordance to PSR model

Specimen	a_1	a_2	R^2
NL	20145	26318	0.9882
NC	251781	-3389	0.9999
HL	37264	13621	0.9987
HC	41252	-19698	0.9991

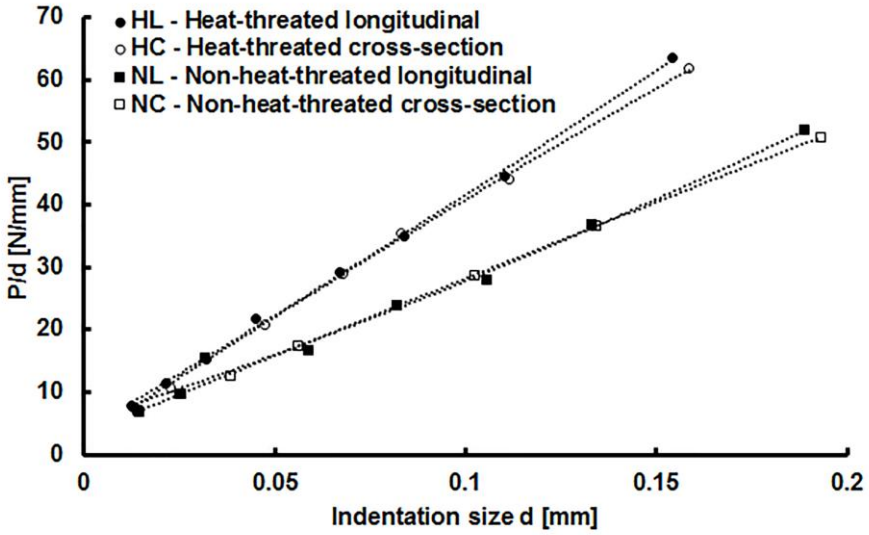

Figure 5. Indentation load versus indentation size according to PSR model

The modified PSR model was proposed by Gong and Li [31]. This behavior model takes into account the existence of surface stress, which may be the result of specimen preparation procedure that encompasses grinding and polishing. This model can be mathematically described in the following manner:

$$P=P_0+a_1d+a_2d^2 \quad (3)$$

where P_0, a_1 and a_2 are experimental constants. The P_0 is a constant related to the surface residual stress associated with surface machining and polishing while a_1 and a_2 have the same meaning as in equation 2 [31]. In the relatively small negative values of P_0 could be expected in case of carefully polished samples [31]. All these parameters are obtained based on load to indentation size fitting curves. The results presented in Table 4 and Fig. 5, of regression analysis, based on the modified PSR model. An excellent fitting is observed with this mathematical model applied, with a correlation factor (R^2) approaching 1, that is, higher than when Meyer's and PSR models were applied. As modified PSR model is considering the surface stresses, a higher correlation factor in modified PSR model results indicate that Knoop microhardness elongated pyramid may be sensitive to the existing surface stresses as P_0 have positive values. Furthermore, a_1 parameter which is associated with elastic behavior, for longitudinal section has negative values (Table 4). This could be attributed to elongated

grains in cross-section (Fig 2b, d) which accommodate larger zone for dislocation movement, thus relaxing surface stress. On the other hand, smaller grains area in in longitudinal section (Fig. 2a, c) reduce dislocation movement and results in presence of residual surface stress. Similar trend can be observed from Table 3, where in cross-sectioned plane (NC and HC) a negative value of a_2 is calculated. As a_2 could be associated with plastic behavior of material, it is evident that there is relaxation of surface stress of elongated grains in cross section.

Table 4 Regression analysis results of the experimental data in accordance to the modified PSR model

Specimen	P_0	a_1	a_2	R^2
NL	13.14	-143.51	28434	0.9994
NC	-1.2949	411.42	24779	1
HL	7.6764	-7.0302	41658	0.9996
HC	-3.98	528.58	36528	0.9999

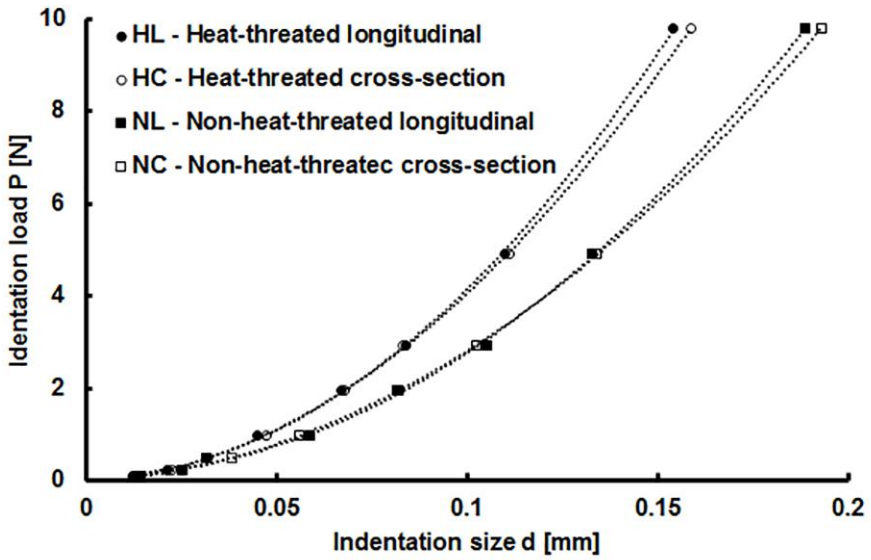

Figure 6. Indentation load versus indentation size according to the modified PSR model

Conclusions

In this paper, the Knoop microhardness method was applied on SLM fabricated specimens, non-heat-treated and heat-treated. Correlation in form of Meyer's law, PSR and modified PSR model were applied to obtained results and the correlation factors were found, to find the most accurate mathematical description of indentation load to indentation size trends. The conclusions are:

Microhardness measured by Knoop indentor in form of an elongated diamond pyramid induces a pronounced indentation size effect (ISE), with a decreased microhardness values as

the loadings are higher. A slightly less pronounced ISE was found in heat-treated specimens, compared to the specimens that were non-heat-treated.
True microhardness or load independent hardness (H_{LIH}) was obtained with minimal Knoop microhardness loading of 2.9 N. This way, H_{LIH} of non-heat-treated specimens was 400 HK, while for heat-treated specimens, it was 600 HK.
In all specimens, when Mayer's, PSR and modified PSR prediction laws were applied, a slightly higher correlation factors are obtained for cross-sectioned specimens with elongated melted areas revealed, compared to the longitudinally sectioned specimens with rounded or scale-like specimens revealed.
The highest correlation factors, approaching 1, were obtained when modified PSR law was applied, followed by Meyer's law and finally by PSR model.
Small difference in hardness behavior in longitudinal and cross-sectioned plane could be associated to the difference in formation of grains, that is, scale-like morphology and elongated grains morphology, respectively.

Acknowledgements:
This paper represents a part of research performed within the project "Advanced design rules for optimal dynamic properties of additive manufacturing products – A_MADAM", which received funding from the European Union's Horizon 2020research and innovation programme under the Marie Skłodowska-Curie grant agreement No.734455.

References:

[1] Deckers J, Meyers S, Kruth JP, et al. Direct selective laser sintering/melting of high density alumina powder layers at elevated temperatures. In: *Physics Procedia*. 2014, pp. 117–124.
[2] Vaezi M, Seitz H, Yang S. A review on 3D micro-additive manufacturing technologies. *Int J Adv Manuf Technol* 2013; 67: 1721–1754.
[3] Akyildiz HK, Kulekci MK, Esme U. Influence of shot peening parameters on high-cycle fatigue strength of steel produced by powder metallurgy process. *Fatigue Fract Eng Mater Struct* 2015; 38: 1246–1254.
[4] Attar H, Calin M, Zhang LC, et al. Manufacture by selective laser melting and mechanical behavior of commercially pure titanium. *Mater Sci Eng A* 2014; 593: 170–177.
[5] Prashanth KG, Scudino S, Klauss HJ, et al. Microstructure and mechanical properties of Al-12Si produced by selective laser melting: Effect of heat treatment. *Mater Sci Eng A* 2014; 590: 153–160.
[6] Buchbinder D, Schleifenbaum H, Heidrich S, et al. High power Selective Laser Melting (HP SLM) of aluminum parts. In: *Physics Procedia*. Elsevier, pp. 271–278.
[7] S. Ćirić-Kostic , N. Bogojević , A. Vranić, D. Croccolo , M. De Agostinis , S. Fini GO. Machining and heat treatment effects on the fatigue properties of Maraging steel produced by DMLS. In: *IX International Conference "Heavy Machinery-HM 2017*. Zlatibor, 2017.
[8] Abe F, Osakada K, Shiomi M, et al. The manufacturing of hard tools from metallic powders by selective laser melting. *J Mater Process Technol* 2001; 111: 210–213.
[9] Shahzad K, Deckers J, Kruth JP, et al. Additive manufacturing of alumina parts by indirect selective laser sintering and post processing. *J Mater Process Technol* 2013; 213: 1484–1494.
[10] Drexler M, Lexow M, Drummer D. Selective Laser Melting of Polymer Powder - Part

Mechanics as Function of Exposure Speed. *Phys Procedia* 2015; 78: 328–336.
[11] Caulfield B, McHugh PE, Lohfeld S. Dependence of mechanical properties of polyamide components on build parameters in the SLS process. *J Mater Process Technol* 2007; 182: 477–488.
[12] Kalentics N, Boillat E, Peyre P, et al. Tailoring residual stress profile of Selective Laser Melted parts by Laser Shock Peening. *Addit Manuf* 2017; 16: 90–97.
[13] Croccolo D, De Agostinis M, Fini S, et al. Fatigue Response of As-Built DMLS Maraging Steel and Effects of Aging, Machining, and Peening Treatments. *Metals (Basel)* 2018; 8: 505.
[14] Croccolo D, De Agostinis M, Fini S, et al. Effects of build orientation and thickness of allowance on the fatigue behaviour of 15–5 PH stainless steel manufactured by DMLS. *Fatigue Fract Eng Mater Struct* 2018; 41: 900–916.
[15] Sanz C, Navas Garcia V, Gonzalo O, et al. Study of surface integrity of rapid manufacturing parts after different thermal and finishing treatments. *Procedia Eng* 2011; 19: 294–299.
[16] Zaeh MF, Ott M. Investigations on heat regulation of additive manufacturing processes for metal structures. *CIRP Ann - Manuf Technol* 2011; 60: 259–262.
[17] Shifeng W, Shuai L, Qingsong W, et al. Effect of molten pool boundaries on the mechanical properties of selective laser melting parts. *J Mater Process Technol* 2014; 214: 2660–2667.
[18] Chlebus E, Kuźnicka B, Kurzynowski T, et al. Microstructure and mechanical behaviour of Ti-6Al-7Nb alloy produced by selective laser melting. *Mater Charact* 2011; 62: 488–495.
[19] Croccolo D, De Agostinis M, Fini S, et al. Influence of the build orientation on the fatigue strength of EOS maraging steel produced by additive metal machine. *Fatigue Fract Eng Mater Struct* 2016; 39: 637–647.
[20] Ryniewicz AM, Bojko Ł, Ryniewicz WI. Microstructural and micromechanical tests of titanium biomaterials intended for prosthetic reconstructions. *Acta Bioeng Biomech* 2016; 18: 111–117.
[21] Campanelli SL, Contuzzi N, Ludovico AD, et al. Manufacturing and characterization of Ti6Al4V lattice components manufactured by selective laser melting. *Materials (Basel)* 2014; 7: 4803–4822.
[22] Zaharia SM, Chicos LA. Mechanical Properties and Corrosion Behaviour of 316L Stainless Steel Honeycomb Cellular Cores Manufactured by Selective Laser Melting. *Trans FAMENA XLI* 2017; 4: 11–24.
[23] Nakamoto T, Shirakawa N, Miyata Y, et al. Selective laser sintering of high carbon steel powders studied as a function of carbon content. *J Mater Process Technol* 2009; 209: 5653–5660.
[24] Nie B, Yang L, Huang H, et al. Femtosecond laser additive manufacturing of iron and tungsten parts. *Appl Phys A Mater Sci Process* 2015; 119: 1075–1080.
[25] Stuers Inc-Ensuring Certainty. Knoop Hardness Testing. *United States - Struers Inc.*, https://www.struers.com/en/Knowledge/Hardness-testing/Knoop# (2018, accessed 4 September 2018).
[26] Swadener JG, George EP, Pharr GM. The correlation of the indentation size effect measured with indenters of various shapes. *J Mech Phys Solids* 2002; 50: 681–694.
[27] Han CS, Hartmaier A, Gao H, et al. Discrete dislocation dynamics simulations of surface induced size effects in plasticity. *Mater Sci Eng A* 2006; 415: 225–233.
[28] Nix WD, Gao H. INDENTITATION SIZE EFFECTS IN CRYSTALLINE MATERIALS: A LAW FOR STRAIN GRADIENT PLASTICITY. *J Mech Phys Solids* 1998; 46: 411–425.

[29] Dobránsky J, Baron P, Simkulet V, et al. Examination of Material Manufactured By Direct Metal Laser Sintering (Dmls). *Metal METABK Slovak Repub E Vojn* 2015; 54: 477–480.
[30] ASTM E 384-08 Standard test method for microindentation hardness of materials. 2008; 1–33.
[31] Gong J, Li Y. Energy-balance analysis for the size effect in low-load hardness testing. *J Mater Sci* 2000; 35: 209–213.
[32] Li H, Bradt RC. The microhardness indentation load/size effect in rutile and cassiterite single crystals. *J Mater Sci* 1993; 28: 917–926.